

Thermodynamic uncertainty relation in helicases: Experiments and simulations

Author: Víctor Rodríguez Franco

Facultat de Física, Universitat de Barcelona, Diagonal 645, 08028 Barcelona, Spain.

Advisor: Maria Mañosas

Felix Ritort Farrán

Abstract: Helicases are molecular motors that translocate on DNA in non-equilibrium conditions and use the energy from ATP hydrolysis to unwind DNA. Here we carry out magnetic tweezers experiments to study the unwinding and translocation activities of the gp41 replicative helicase in a DNA hairpin under the effect of a mechanical force. We analyze the experimental results to compute the mean helicase rate and the diffusion coefficient in different experimental conditions (forces and ATP concentration). These quantities are related to the thermodynamic uncertainty factor Q [1], which can be used as a measure of the irreversibility of a given enzymatic process. We find that the Q factor decreases with the applied force and has a non-monotonic behaviour with the ATP concentration. The results are compared with simulations of a simple model based on a biased random walk to describe the helicase motion on DNA.

I. INTRODUCTION

Helicases are proteins that use the energy from ATP hydrolysis to separate the two strands of the DNA double-helix, a reaction required in many cellular processes (e.g. DNA replication). They catalyse the DNA unwinding reaction by lowering the activation barrier via the conversion of chemical energy from ATP hydrolysis into mechanical work, acting as a molecular motor. The unwinding process is essential for DNA replication where the double helix is separated into two single stranded DNA chains by the helicase, then another enzyme (polymerase) is hooked in the single strand and begins to copy the DNA, leading to two identical DNA molecules.

The energies involved in the unwinding reaction, i.e the energy of breaking a DNA base-pair and the energy from ATP hydrolysis, are on the order of few $k_B T$. Therefore helicases work in strong Brownian environment. In their out of equilibrium activity they incur thermodynamic costs (dissipation). The recently derived thermodynamic uncertainty relation [1–3] relates the dissipation and fluctuations in the activity of helicases, through the Q factor, as:

$$Q = \sigma_{tot} \frac{2D}{v^2} = S_{bp} \frac{2D}{v} \geq 2, \quad (1)$$

where v is the mean motor velocity, D is the diffusion coefficient and σ_{tot} is the entropy production rate (in k_B units), which can be written as the product of the mean entropy production per unwound base-pair, S_{bp} , times v . Note that we have taken the Boltzmann's constant k_B equal one in Eq. 1, and so the Q factor is in k_B units.

In this work we have performed experiments with a replicative helicase using magnetic tweezers. By manipulating a DNA hairpin and applying a mechanical force at their extremities (on the pN range), we can measure the DNA extension (on the nm range). The measured extension can be used as a reaction coordinate to follow the unwinding reaction (FIG.1). These experiments allow to follow in real time the activity of single helicase

unwinding of a DNA molecule. From the statistics of the unwinding traces and analyzing the mean and the variance of the helicase displacement, we can measure the mean unwinding velocity and diffusion constant and estimate the Q factor in Eq. 1. We have done experiments in different conditions, varying the external applied force and the ATP concentration in order to investigate how these conditions affect the value of the Q factor. Furthermore, we have used a simple biased random walk to describe the helicase motion on a DNA chain. We have performed simulations of this simple model in the different experimental conditions tested to compare them with experimental results.

II. SETUP AND METHODS

A. Magnetic tweezers and experiments

The magnetic tweezers set up is schematically depicted in Fig.1 A. We prepare micron-sized magnetic beads that are attached to a DNA hairpin via biotin-streptavidin interactions [4]. To carry out experiments, we inject the beads with DNA into a microfluidic channel illuminated from above by a LED. The beads are visualized via an inverted microscope connected to a CCD camera. The parallel illumination produce diffraction rings and analyzing these rings we can track the 3D position of each bead in real time [5]. One extremity of the DNA hairpin is labeled with digoxigenin that binds the anti-digoxigenin treated surface of the microfluidic channel. The tethered DNA molecule is then stretched by using a pair of magnets located on top of the channel. The value of the applied force can be controlled by changing the position of the magnets relative to the channel (i.e. the bead feels a greater force the closer it is to the magnets, ranging forces from 10^{-3} to 100 pN [4]).

By adding the gp41 helicase (replicative helicase from T4 bacteriophage) and ATP into the channel we can

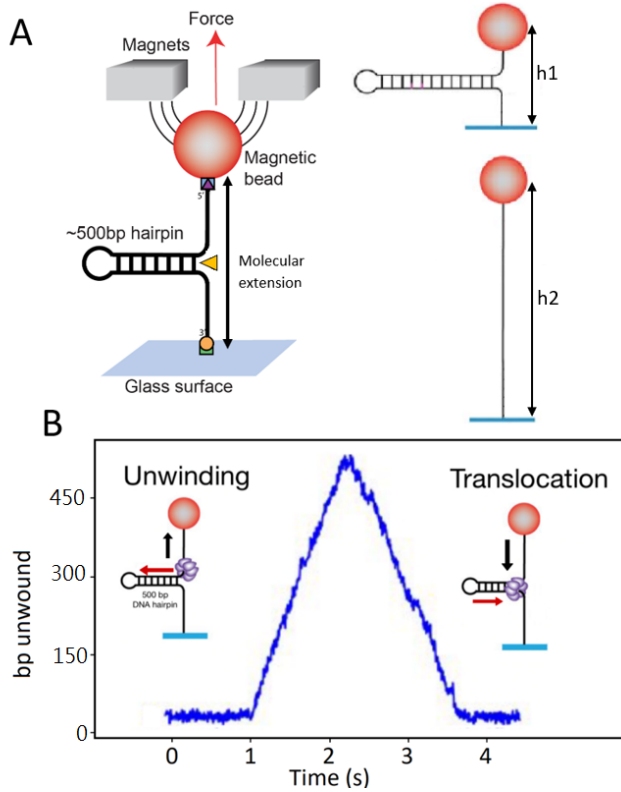


FIG. 1: (A) Schematic representation of the magnetic tweezers with a DNA hairpin tethered between the magnetic bead and the channel surface. The helicase (in yellow) unwinds the hairpin leading to an increase of the molecular extension. (B) Experimental trace showing full unwinding of the hairpin (rising edge) followed by the translocation of the helicase on the single stranded unwound DNA while the hairpin rezzips in its wake (falling edge). Red arrows indicate gp41 motion and black arrows indicate bead motion.

follow the gp41 unwinding reaction by measuring the changes in DNA extension: initially the hairpin is formed and the bead is at height h_1 ; next when the helicase opens the hairpin, the DNA lengthens and the bead moves at $h_2 > h_1$ (FIG.1A). Experimental traces show an increase on the DNA extension corresponding the helicase DNA unwinding until the hairpin is fully unzipped (FIG.1B). Next, the extension decreases corresponding to the helicase translocation on the single-stranded DNA while the hairpin rezzips in its wake. The position is measured with a precision of nm and the program allows us to track different beads at the same time, being able to have a lot of statistics in a single experiment [5]. The extension in nm can be converted to number of unwound base-pairs by using the previously measured elasticity of single-stranded DNA [6, 7].

The experiments were carried out using a ~ 500 base-pair (bp) hairpin at 25°C in 10mM MgCl₂ buffer with 60nM gp41 helicase. The acquisition frequency was 300Hz. We tested different experimental conditions. First, we fixed the height of the magnets (constant force) and changed

the ATP concentration, from low concentration to high concentration (ATP saturating conditions). Second, at high ATP condition (8mM), we tested the helicase unwinding activity at different external forces (from 5 to 13 pN).

B. Model and simulations

In this study, we use a biased random walk to describe the motion of the helicase on the DNA during unwinding [8]. In this model, the probability of the motor to be in the base n along the DNA chain, p_n , is given by $dp_n/dt = k^+ p_{n-1} + k^- p_{n+1} - (k^+ + k^-) p_n$ with different rates k^+ and k^- of moving forward and backwards. The helicase dynamics is then determined by the rates k^+ and k^- , given by:

$$k^+ = k_0 \exp\left(\frac{-\Delta G_{bp} + W_{net}}{k_B T}\right) \quad (2)$$

$$k^- = k_0 \exp\left(\frac{-\Delta\mu}{k_B T}\right) \quad (3)$$

where k_0 is an attempt frequency, ΔG_{bp} is the free energy of base-pair formation, $\Delta\mu$ is the energy coming from the ATP hydrolysis and W_{net} is the net work done by the force. Note that these rates verify the detail balance condition since that total change in free energy between two consecutive positions (n and $n+1$) of the motor in the DNA chain is given by $\Delta G_T = \Delta\mu - \Delta G_{bp} + W_{net}$. The mechanical work W_{net} is calculated following the worm-like chain model (WLC) which assumes that the polymer is a semi-flexible rod with a force-extension relation [9] given by:

$$F = \frac{k_B T}{P} \left[\frac{1}{4} \left(1 - \frac{x}{L}\right)^{-2} - \frac{1}{4} + \frac{x}{L} \right] \quad (4)$$

where x is the polymer extension, P the persistence length, L the contour length and F the external force. The conversion from nm to unwound base-pairs at each force can be obtained from this equation for a contour length corresponding to only one base (e.g $L = l = 0.69$ nm). Using this elastic model, the net work reads as:

$$W_{net} = \Delta x \left[F - \frac{1}{P\beta\delta} \left(\frac{l^2}{2l - \delta} - \frac{\delta + 2l}{4} + \frac{\delta^2}{4l} \right) \right] \quad (5)$$

where l is the length of one base and δ is the nm/bp conversion factor.

From the simulations we can compute the velocity and the diffusion constant. For constant rates k^+ and k^- the biased-random model can be solved [8] leading to:

$$D = \frac{k^+ + k^-}{2} \quad , \quad v = k^+ - k^- \quad (6)$$

We have first confirmed that our simulations verified these relations for the case where the force, ATP concentration and ΔG_{bp} are fixed. This latter case would correspond to an homogeneous DNA sequence (with a single base-pair type). In order to take into account the heterogeneous sequence of the hairpin used in the experiments, we have used the nearest-neighbour base-pair energies [10] to calculate the energy associated to each individual base-pair in the sequence. Simulations from the real DNA sequence and homogeneous sequence (with the $\Delta G_{bp} = 2.62k_B T$ equal to the mean ΔG_{bp} of the real sequence) are compared.

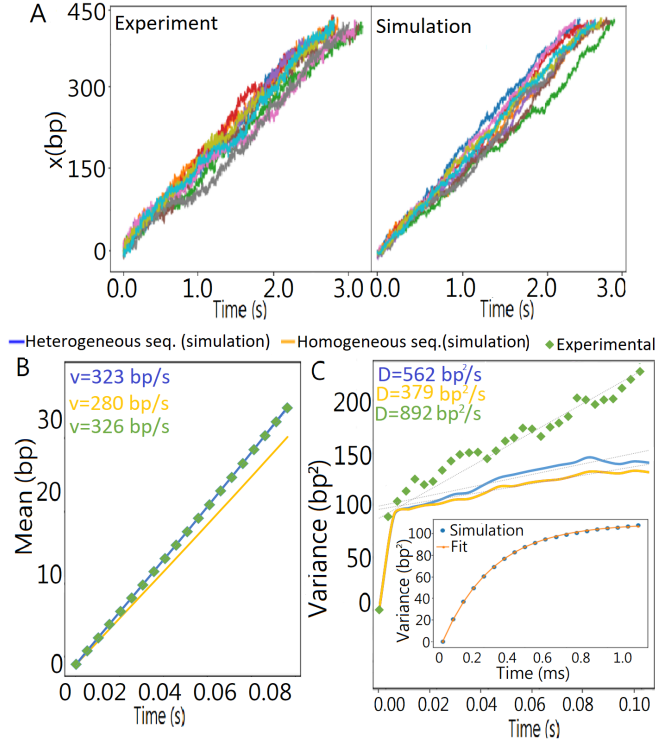


FIG. 2: (A) Comparison between experimental (left panel) and simulated (right panel) unwinding traces. (B) The mean unwinding rate is obtained from the lineal fit to the mean helicase displacement from experiments (green) and from simulations of the biased random walk (Eq. 2,3) in a homogeneous (orange) and heterogeneous (blue) sequence coupled to the bead dynamics (Eq. 7). The prefactor $k_0 = 50\text{s}^{-1}$ used in simulations is chosen to match the experimental unwinding velocity for the heterogeneous case. (C) The variance as a function of time showing linear and exponential behaviour for both experimental and simulation results (colors as in panel B). The linear fit gives information about the diffusion coefficient, leading to larger D values for experiments than for simulations. Inset show details of the non-linear regime, with the fit to Eq. 8

In order to simulate the experimental conditions, we have also included in the simulations the Brownian motion of the bead. We consider that the bead position x follows a Langevin dynamics of an overdamped particle (i.e., without inertial term), given by:

$$\gamma dx/dt = F - k_{ssDNA} x + \xi \quad (7)$$

Where DNA is considered as an elastic spring of stiffness k_{ssDNA} , and the noise term ξ is a white noise with zero mean and standard deviation $\sigma = \sqrt{2k_B T \gamma}$, with γ the drag coefficient of the bead.

III. RESULTS

A. Helicase displacement analysis

We have performed simulations of the unwinding activity of the helicase motor working on a DNA molecule coupled to a micron-sized bead. The simulations are performed for both a homogeneous sequence (with all base-pairs having the same energy) and a heterogeneous sequence (the sequence we used in the experiment). We have compared the simulation results with the experimental ones obtained with the gp41 helicase using magnetic tweezers. FIG.2A shows the unwinding traces obtained in experiments and simulations. For both experiments and simulations we compute the mean and the variance of the measured displacement x for a given time interval t , finding a lineal time dependence for both: $\langle x \rangle = vt$ and $\langle x^2 \rangle = 2Dt$ (FIG.2B-C). For the homogeneous sequence simulations, the values for D and v agree with the expected ones given by Eq. 6 for $t > \tau$. At shorter times ($t < \tau$) we observe an exponential behaviour for both simulation and experimental results (FIG.2C). This can be interpreted as a sub-diffusive regime where the motor has not opened many bases and the dynamics is governed by the fluctuations of the bead. Once the motor has moved some bases forward, the sub-diffusive regime ends and the behaviour is lineal, i.e. diffusive. The mean square displacement of the bead-motor system is given by:

$$\sigma^2 = 2\sigma_{bead}^2 (1 - e^{-t/\tau}) + 2Dt \quad (8)$$

where σ_{bead} is the fluctuations of the bead (without motor) and τ the bead relaxation time. Therefore the extrapolation of the lineal behaviour of σ^2 to zero time gives information about the bead fluctuations. Fitting the exponential expression at ($t < \tau$) we obtain $\tau = 0.0003\text{s}$ (Inset FIG.2C), which coincides with the inverse of the corner frequency of the bead ($\omega_c \approx 3\text{kHz}$).

The simulations for homogeneous and heterogeneous sequences lead to similar results, but the values for D and v for the heterogeneous case are closer to the experimental results. However, the diffusion constant measured experimentally is significantly larger than that obtained in simulations (FIG.2C).

B. Force and ATP dependencies

Experiments and simulations were carried out at different applied forces, ranging from 5 to 13 pN. In both cases, we measure a mean rate that increases with the force (FIG.3 top panel). This result is expected, since force destabilizes the DNA base-pairs, decreasing the effective barrier for DNA unwinding. This is included in the model by the W_{net} term in the rates in Eq. 2. The fact that the unwinding rate of gp41 increases with the applied force has been previously reported and associated to the passive character of this helicase [6, 7]. However, the helicase diffusivity was not previously studied.

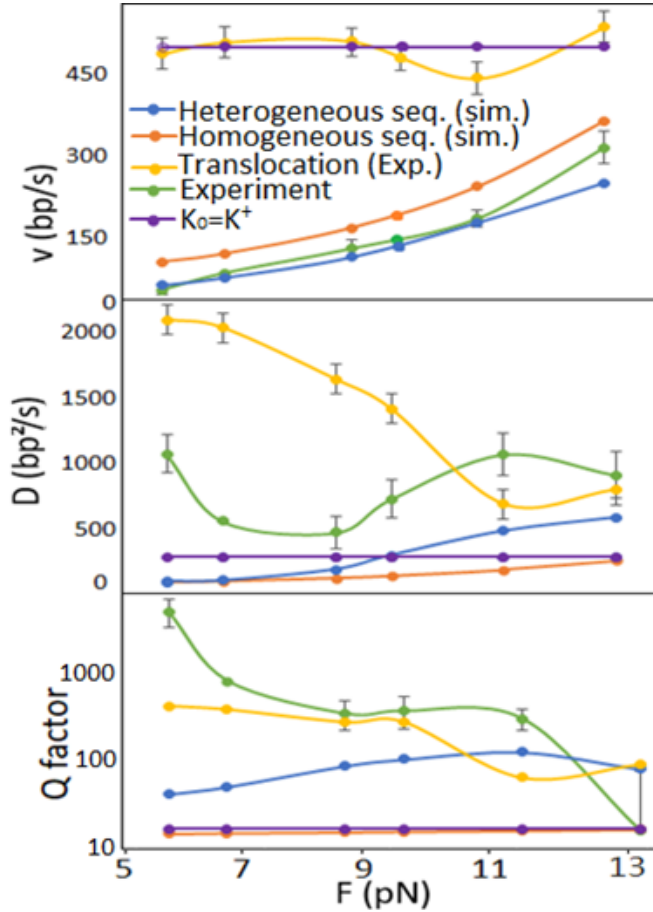


FIG. 3: Results of the mean rate (v), the diffusion (D) and the Q factor extracted from the experimental data (unwinding and translocation) and the simulation with an homogeneous and heterogeneous sequence. Simulations reproduce well the rate dependence on force. But they fail to explain the results for the diffusion and Q factor.

From the variance analysis, simulations predict a diffusion constant that increases with the applied force, with larger D values for the heterogeneous case (FIG.3 central panel). The experimental results show a diffusion constant that does not exhibit a monotonic behavior with force and it is between 2 and 10 times larger than those obtained from simulations. The bigger differences are

observed at low forces (FIG.3 central panel). For the translocation activity we obtain a constant translocation rate. This result agrees with an scenario in which the forward rate is independent of the force, $k^+ = k_0$. However, in this latter case the diffusion constant (and also the Q factor) would be constant and we measure a diffusion constant (and a Q factor) that decreases with force (FIG.3 central panel).

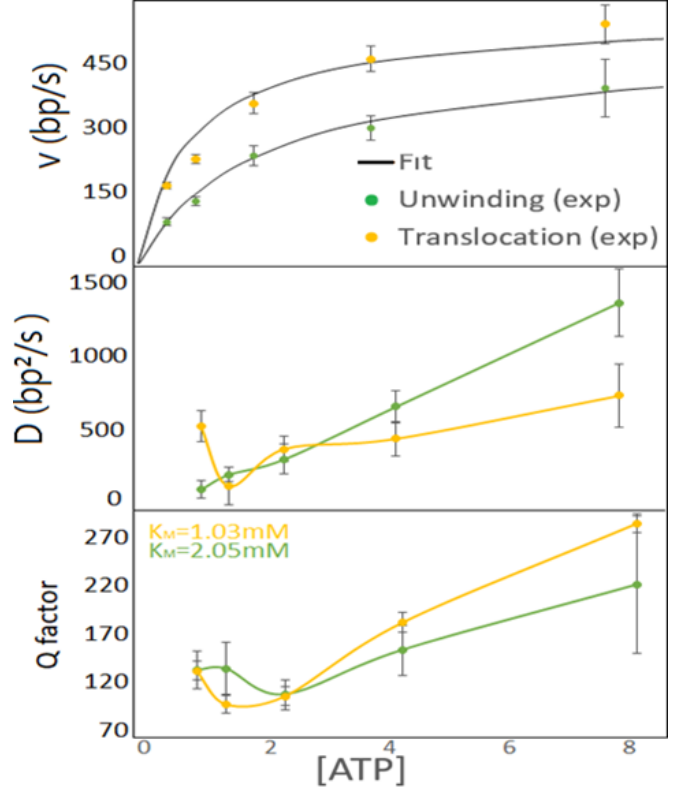


FIG. 4: Experimental results for the ATP dependence. The mean unwinding and translocation rates follow a Michaelis-Menten dependence with the ATP concentration. Fits are shown as continuous lines with $K_M=2.05\pm 0.01\text{mM}$ and $v_{max}=461\pm 50\text{ bp/s}$ for unwinding and $K_M=1.03\pm 0.02\text{mM}$ and $v_{max}=611\pm 7\text{ bp/s}$ for translocation. The Diffusion constant increases with [ATP] and the Q factor has a minimum near K_M .

From the measurements of v and D we estimate the Q factor (Eq.1) by using an entropy production per unwound base-pair given by: $S_{bp} = \Delta\mu - \Delta G_{bp} + W_{net}$. This entropy production is computed assuming a tight mechano-chemical coupling of one base-pair unwound per ATP, which is the case for many DNA helicases [11, 12]. Note that the energy of ATP hydrolysis is very large as compared to the other energetic terms ($\Delta\mu \sim 25k_B T$, whereas $\Delta G_{bp}, W_{net} \leq 3k_B T$). Therefore $k^+ \gg k^-$ and the enzyme can be considered as unidirectional. In these conditions, the ratio between $2D$ over v is equal to 1 for an homogeneous sequence, giving a Q factor that only depends on the entropy production per unwound base-pair and it is almost constant $Q = S_{bp} \sim \Delta\mu$, bottom

panel of FIG.3. For the heterogeneous sequence the Q factor is larger and increases slightly with the force. For the experimental results, the Q factor is much larger and decreases with the applied force (FIG.3 botom panel).

We have also carried experiments at 12pN and at different ATP concentrations, from 500 μ M to 8 mM and measured the mean helicase rate and diffusivity. The mean unwinding velocity increases with ATP concentration, reaching a saturated value near to $[ATP]=8$ mM. The velocity versus $[ATP]$ results can be fitted the Michaelis-Menten equation $v = \frac{v_{max}[ATP]}{K_M+[ATP]}$ where v_{max} is the maximum velocity obtained in the saturated ATP condition and K_M is the Michaelis-Menten constant (FIG.4 top panel). From the fit we get $K_M=2.05$ mM. For the diffusion constant we also observe an increasing behaviour as we increase the ATP concentration (FIG.4 central panel). Comparing these two factors we can calculate the Q factor that shows a minimum near a $[ATP] \approx K_M$ and increase till the saturation value (FIG.4 bottom panel). This result was predicted from theoretical studies [3] but it was not measured before.

The translocation results show similar trend for the velocity (with lower k_M of 1.03 mM), the diffusion constant and the Q factor.

IV. CONCLUSIONS

We have performed magnetic tweezers experiments to investigate the unwinding and translocation activity of a replicative helicase. From the experimental traces we have measured its rate and diffusivity in different experimental conditions (different forces and $[ATP]$). These measurements allowed us to estimate the ratio between dissipation and fluctuations (defined as a Q factor) in

the activity of this motor. We find that the Q factor depends on the experimental conditions decreasing with the force and having a non-monotonic behaviour with $[ATP]$, presenting a minimum located in the Michaelis-Menten constant in agreement with theoretical predictions [3]. However the Q values we measured, ranging from 10 to 10^3 depending on force and ATP concentration, are a bit larger than those predicted for other molecular motors ($Q \sim 10$) [3].

We have also modeled the experiments using a simple biased random walk for describing the helicase motion along the DNA chain and including the dynamics of the bead tethered to the DNA molecule. Simulations of the model qualitatively reproduce the experimental traces and the force dependence of the mean unwinding and translocation rates. However, the diffusivity of the model differs significantly from the experiments and so the Q factor. We conclude that the model is too simple to describe the complexity of the helicase unwinding and translocation reaction. We envision to extend the model in two directions: 1) include the ATP hydrolysis reaction and consider different types of mechano-chemical couplings and 2) include an helicase off-pathway pausing state that could explain the force dependence of the unwinding and translocation diffusion constant D .

Acknowledgments

I would like to thank Small Biosystems Lab for providing the laboratory and their help whenever I've needed. I would like to express my deepest gratitude to my advisor M. Mañosas who has given me the opportunity to discover a new way of doing physics. A special thanks to my family and Emma for their support and time.

-
- [1] Barato, A. C., & Seifert, U. (2015). Thermodynamic uncertainty relation for biomolecular processes. *Physical review letters*, 114(15), 158101.
 - [2] Pietzonka, P., Ritort, F., & Seifert, U. (2017). Finite-time generalization of the thermodynamic uncertainty relation. *Physical Review E*, 96(1), 012101.
 - [3] Song, Y., & Hyeon, C. (2021). Thermodynamic uncertainty relation to assess biological processes. *The Journal of Chemical Physics*, 154(13), 130901.
 - [4] Lionnet T., Allemand J. F., Revyakin A., Strick T. R., Saleh O. A., Bensimon D. & Croquette V. (2011). Single-Molecule Studies Using Magnetic Traps. *Cold Spring Harbor Protocols*.
 - [5] Gosse, C., & Croquette, V. (2002). Magnetic tweezers: micromanipulation and force measurement at the molecular level. *Biophysical journal*, 82(6), 3314-3329.
 - [6] Manosas, M., Xi, X. G., Bensimon, D., & Croquette, V. (2010). Active and passive mechanisms of helicases. *Nucleic acids research*, 38(16), 5518-5526.
 - [7] Lionnet, T., Spiering, M. M., Benkovic, S. J., Bensimon, D., & Croquette, V. (2007). Real-time observation of bacteriophage T4 gp41 helicase reveals an unwinding mechanism. *Proceedings of the National Academy of Sciences*, 104(50), 19790-19795.
 - [8] Berg, H. C. (2018). *Random walks in biology*. Princeton University Press.
 - [9] Bouchiat, C., Wang, M. D., Allemand, J.-F., Strick, T., Block, S. M., & Croquette, V. (1999). Estimating the Persistence Length of a Worm-Like Chain Molecule from Force-Extension Measurements. *Biophysical Journal*, 76(1), 409-413.
 - [10] Huguet, J. M., Ribezzi-Crivellari, M., Bizarro, C. V., & Ritort, F. (2017). Derivation of nearest-neighbor DNA parameters in magnesium from single molecule experiments. *Nucleic Acids Research*, 45(22), 12921-12931.
 - [11] Sun, B., Johnson, D. S., Patel, G., Smith, B. Y., Pandey, M., Patel, S. S., & Wang, M. D. (2011). ATP-induced helicase slippage reveals highly coordinated subunits. *Nature*, 478(7367), 132-135.
 - [12] Xie, P. (2020). Non-tight and tight chemomechanical couplings of biomolecular motors under hindering loads. *Journal of theoretical biology*, 490, 110173.